PNAS
www.pnas.org

Supplementary Information for

GDF11 promotes osteogenesis as opposed to MSTN, and follistatin, a MSTN/GDF11 inhibitor, increases muscle mass but weakens bone

Joonho Suh[1], Na-Kyung Kim[1], Seung-Hoon Lee[2], Je-Hyun Eom[1], Youngkyun Lee[3], Joo-Cheol Park[4], Kyung Mi Woo[1], Jeong-Hwa Baek[1], Jung-Eun Kim[2], Hyun-Mo Ryoo[1], Se-Jin Lee[5,6], Yun-Sil Lee[1,*]

Corresponding author: Yun-Sil Lee
Email: yunlee@snu.ac.kr

This PDF file includes:

Other supplementary materials for this manuscript include the following:

www.pnas.org/cgi/doi/10.1073/pnas.1916034117

Supplementary methods

Mice. All mice were maintained on a C57BL/6 background. Generation of *Gdf11* conditional knockout mice has been previously described (1). *Cdx2-Cre* male mice and *CAG-Cre-ER* male mice were purchased from the Jackson Laboratory (Bar Harbor, ME). *Mstn* null mice have been previously described (2). *Prx1-Cre* mice were kindly provided by Youngkyun Lee (Kyungpook National University School of Dentistry, Republic of Korea). *F66* mice have also been formerly described (3). To analyze E18.5 embryos, *Gdf11*$^{flox/flox}$ females mated with *CAG-Cre-ER*; *Gdf11*$^{flox/flox}$ males were administered with 4-hydroxytamoxifen (Sigma) intraperitoneally at a dose of 0.7 mg/day for 3 consecutive days, starting from E7.5. To analyze young adult mice, 4-week-old male littermates obtained from the mating between *CAG-Cre-ER*; *Gdf11*$^{flox/flox}$ males and *Gdf11*$^{flox/flox}$ females were injected with tamoxifen (Sigma) at a dose of 75 mg/kg/day for 5 consecutive days. All animal studies were approved by the Institutional Animal Care and Use Committees at Seoul National University.

MicroCT analysis. MicroCT analysis was performed using Skyscan 1172, 1272, 1275 (Bruker-MicroCT), and inspexio SMX-90CT (Shimadzu) following the manufacturers' guidelines (method notes provided by Bruker). Skyscan 1272 was used exclusively for the representative images of T3 and L1 of newborn mice, which were taken with a pixel size of 4 μm at 50 kV and 200 μA through no filter. Skyscan 1275 was used to scan whole skeletons of newborn and E18.5 mice. Scans were performed with a pixel size of 10 μm at 40 kV and 250 μA through no filter. Skyscan 1172 was used to scan and analyze T3 and L1 of newborn and E18.5 mice. Scans were performed with a pixel size of 4 μm at 50 kV and 200 μA through no filter. Region of interest (ROI) for the vertebral bodies of newborn mice and embryos were obtained using the "ROI shrink wrap" function in CTAn (v1.17.7.2), a manufacturer-provided software. Skyscan 1275 was used with a pixel size of 10 μm at 60 kV and 160 μA through no filter for adult vertebrae, a pixel size of 10 μm at 50 kV and 200 μA through no filter for 10-week-old mouse tibias, and a pixel size of 10 μm at 50 kV and 200 μA through 1 mm aluminum filter for 5- and 6-week-old mouse humerus. ROI for the vertebral trabecular bone was initially set as a circle with 2 mm diameter. Subsequently ROI was determined automatically using the "ROI shrink wrap," "bitwise operations," and "morphological operations" functions in CTAn. Vertebral trabecular bones 0.5 mm away from each growth plates were analyzed. For proximal and distal cortical analysis of tibias, 1 mm of bone (in height) was analyzed for each group. For humerus, trabecular bones from 0.2 mm away from the growth plate to the distal end of deltoid tuberosity were analzed. One mm of distal cortical bone of the humerus located below deltoid tuberosity was analyzed. Lugol's solution (Sigma) was used to enhance soft tissue contrast as previously described (4). Images were reconstructed and displayed using manufacturer-provided software NRecon (v1.7.3.2), CTvox (v3.3.0), and CTvol (v2.3.2.0). For supplementary

figure images produced using inspexio SMX-90CT, TRI/3D-BON (RATOC System) software was used for 3D reconstruction.

Bone hisotomorphometry analysis. Calcein and alizarin red S labeling, von Kossa, and tartrate-resistant acid phosphatase (TRAP) staining on tissue sections were performed as previously described with slight modifications (5). For calcein and alizarin red S labeling, mice were first intraperitoneally injected with calcein green (15 mg/kg; Sigma) and subsequently with alizarin red S (60 mg/kg; Sigma) 4 days later, and were sacrificed 2 days after the final injection. Five μm sections of L1 vertebrae and tibia were prepared after fixation, dehydration, and embedding in destabilized methyl-methacrylate. TRAP staining using Leukocyte TRAP Kit (Sigma) was performed on decalcified tibia sections after dehydration and paraffin embedding. Bone histomorphometry analyses were performed using BioQuant software (Bio-Quant). Newborn mouse vertebrae were frozen in O.C.T. compound (Tissue-Tek) and 18 μm frontal sections were stained in H&E.

DXA analysis. Young adult male mice were anesthetized by inhalation of isoflurane (Aerane, Baxter) and were scanned using InAlyzer (Medikors). Images were generated through manufacturer-provided digital imaging software InAlyzer.

Osteoblast culture and differentiation. Osteoblasts were isolated from newborn mouse calvaria as previously described (6). Briefly, calvaria was dissected and sequentially incubated in digestion solution containing 0.2% (w/v) type II collagenase (Worthington). Afterwards, the cells were pooled and cultured for 3 days until confluence in α-MEM containing 10% FBS and 1% penicillin/streptomycin. Osteoblasts were differentiated by the addition of 5 mM β-glycerophosphate (Sigma) and 50 μg/ml ascorbic acid (Sigma) to the culture medium and half of the medium was changed every 3 days. Seven days after differentiation, cells were fixed with 4% paraformaldehyde and stained for ALP as previously described (7). ALP activity was evaluated using StemTAG Alkaline Phosphatase Activity Assay Kit (Cell Biolabs) according to the manufacturer's recommendations. Fourteen days after differentiation, cells were fixed with 4% paraformaldehyde and stained with 2% ARS solution (pH 4.2, Sigma) for 15 minutes (8).

Chondrocyte culture and maturation. Chondrocytes were isolated from newborn mouse costal cartilage as previously described (9). In short, costal cartilage was isolated and sequentially incubated in 0.2% (w/v) pronase (Sigma) and 0.3% (w/v) type IV collagenase (Gibco) solutions. The cells were pooled, seeded at high density (100,000 cells/cm^2), and cultured until confluence in DMEM containing 10% FBS and 1% penicillin/streptomycin. Chondrocyte maturation was induced by the addition of 5 mM β-glycerophosphate (Sigma) and 50 μg/ml ascorbic acid (Sigma) to the

culture medium. Seven days after differentiation, cells were fixed with 4% paraformaldehyde and stained for ALP as previously described (7). ALP activity was evaluated using StemTAG Alkaline Phosphatase Activity Assay Kit (Cell Biolabs) according to the manufacturer's recommendations. Cells were also stained with 1% Alcian Blue solution (Alcian Blue 8 GX, Sigma, in 0.1N HCl) for 30 minutes (10).

Osteoclast differentiation and resorption assay. Splenocytes were isolated from newborn mouse spleen as previously demonstrated (11) with slight modifications. Briefly, newborn mouse spleen was gently crushed with the back of a syringe plunger, suspended in medium, and filtered. After centrifugation, the cell pellet was dissolved in Red Blood Cell Lysis Buffer (Sigma), incubated for 5 minutes on ice, and washed by centrifugation with medium. The cells were resuspended in α-MEM containing 10% FBS, 1% penicillin/streptomycin, and 25 ng/ml MCSF (Peprotech), and cultured overnight. Subsequently, non-adherent cells were collected and plated at 50,000 cells/cm^2 in culture medium supplemented with 50 ng/ml MCSF and 50 ng/ml RANKL (Peprotech). Four days after differentiation, osteoclasts were fixed with 4% paraformaldehyde and stained for TRAP using TRAP Staining Kit (Cosmo Bio) according to the manufacturer's recommendations. Pit formation and resorption activity were measured using Bone Resorption Assay Kit (Cosmo Bio) containing calcium phosphate-coated plates. Osteoclast/pit size and number were calculated using Zen 2.3 pro software (Zeiss), and osteoclast activity was evaluated through Spark 10M (Tecan).

Overexpression. Full-length human *GDF11*, *MSTN* (provided by Se-Jin Lee), and mouse *Inhba* cDNAs (Origene) were cloned into pcDNA3.1(+) vector. Plasmids (1 μg) were reverse transfected into primary osteoblasts seeded in a 12-well plate using TransIT-LT1 transfection reagent (Mirus Bio).

siRNA Transfection. Predesigned siRNAs purchased from Bioneer (Korea) were reverse transfected to primary osteoblasts derived from newborn mouse calvaria at a final concentration of 30nM using Lipofectamine RNAimax (Invitrogen) according to the manufacturer's guideline. The same method was used to reverse transfect non-adherent primary splenocytes (50,000 cells/cm^2) in culture medium supplemented with 50 ng/ml MCSF and 50 ng/ml RANL (Peprotech). siRNA IDs are listed as follows: 14651-1 for si*Gdf11*; 17700-1 for si*Mstn*; 16323-1 for si*Inhba*; 17125-1 for si*Smad1*; 17126-1 for si*Smad2*; 17127-1 for si*Smad3*; 17128-1 for si*Smad4*; 17129-1 for si*Smad5*; 55994-1 for si*Smad9*. The catalogue number for siCtrl is SN-1001-CFG.

Quantitative RT-PCR. Total RNA was extracted from cells using QIAzol Lysis Reagent (Qiagen), and cDNA was prepared using PrimeScript RT Reagent Kit (Takara) according to the manufacturers' protocol. Quantitative RT-PCR was performed using TB Green Premix Ex Taq

(Takara) and StepOnePlus Real-Time PCR system (Applied Biosystems). Relative gene expression was determined using standard $2^{(-\Delta\Delta Ct)}$ calculations by normalizing to 18S rRNA. Primers used in this study are listed in Table S1.

Western blot. Cells or tissues were lysed using Pro-Prep (Intron Biotechnology) lysis buffer supplemented with PhosSTOP (Roche) phosphatase inhibitor cocktail. The samples were denatured at 100°C for 5 minutes in sample buffer (Cure Bio) and separated on 10% SDS-polyacrylamide gels. The proteins were transferred to polyvinylidene difluoride membranes, blocked with 5% BSA for 1 hour and incubated with primary antibodies overnight. The primary antibodies used are listed as follows: rabbit anti-phospho-Smad1/5/9 (1:1000; #13820; Cell Signaling), rabbit anti-Smad1/5/8 (1:1000, sc-6031-R, Santa Cruz), rabbit anti-phospho-Smad2/3 (1:1000, #8828, Cell Signaling), and β-Actin (C4) HRP (1:1000, sc-47778 HRP, Santa Cruz). After incubation with horseradish peroxidase-conjugated anti-rabbit IgG (Invitrogen), signals were detected using SuperSignal reagents (Thermo Scientific).

Embryo analysis. Alcian blue/alizarin red staining of E15.5 and E18.5 embryo skeletons were performed as previously described (12).

Fluorescence and confocal microscopy. LSM 800 confocal microscope (Zeiss) was used to image GFP positive cells in E9.5 *Cdx2-Cre; Gdf11*$^{flox/+}$*; Igs1*$^{CKI\text{-}mitoGFP/+}$ embryos and 4-week-old *Cdx2-Cre; Gdf11*$^{flox/+}$*; Igs1*$^{CKI\text{-}mitoGFP/+}$ mice calvarial bones after mounting with Fluoroshield with DAPI (Sigma).

Statistics. All statistical analysis was performed using SPSS version 23 (IBM Corporation). Two groups were compared by two-tailed Student's *t* test, and multiple groups were compared by ANOVA with Tukey's *post hoc* test. All data represent means ± SEM. A value of $P < 0.05$ was considered statistically significant.

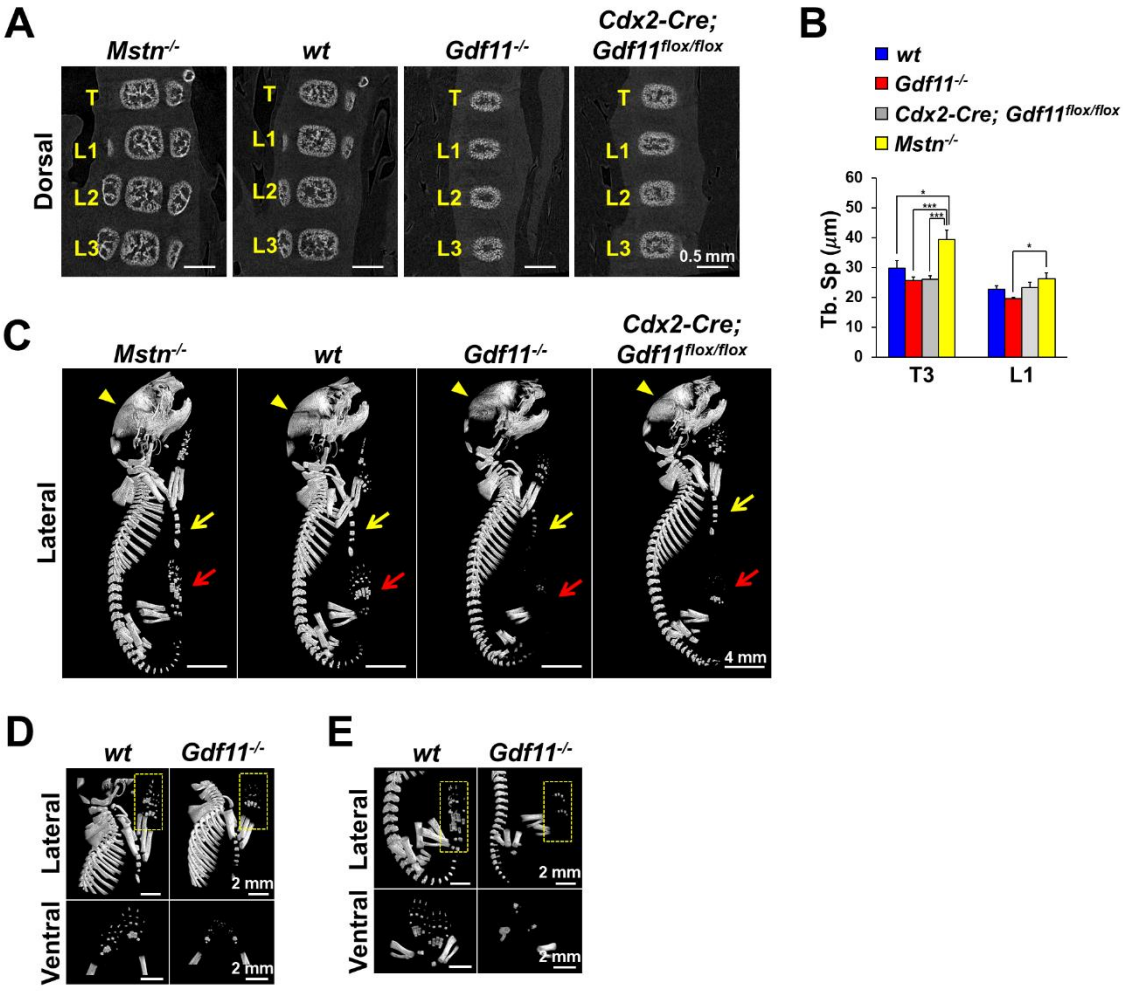

Fig. S1. *Gdf11* deletion decreases bone mass in contrast to *Mstn* deletion. (*A*) Raw microCT cross section images (scanned with Skyscan) of newborn mouse vertebrae. (*B*) Supplemental microCT histomorphometric analysis (Tb. Sp, Trabecular separation) to Fig. 1*D*. (*C*) Representative microCT images (scanned with Skyscan) of lateral view of newborn mouse skeletons. Yellow arrowheads, yellow arrows, and red arrows indicate calvarial bones, sterna, and hindlimb autopods, respectively. (*D* and *E*) Representative microCT images (scanned with Skyscan) of newborn mouse limbs. Yellow boxed regions in (*D*) and (*E*) are rotated to display ventral views of forelimb and hindlimb autopods, respectively. All scale bars are displayed with actual size values.

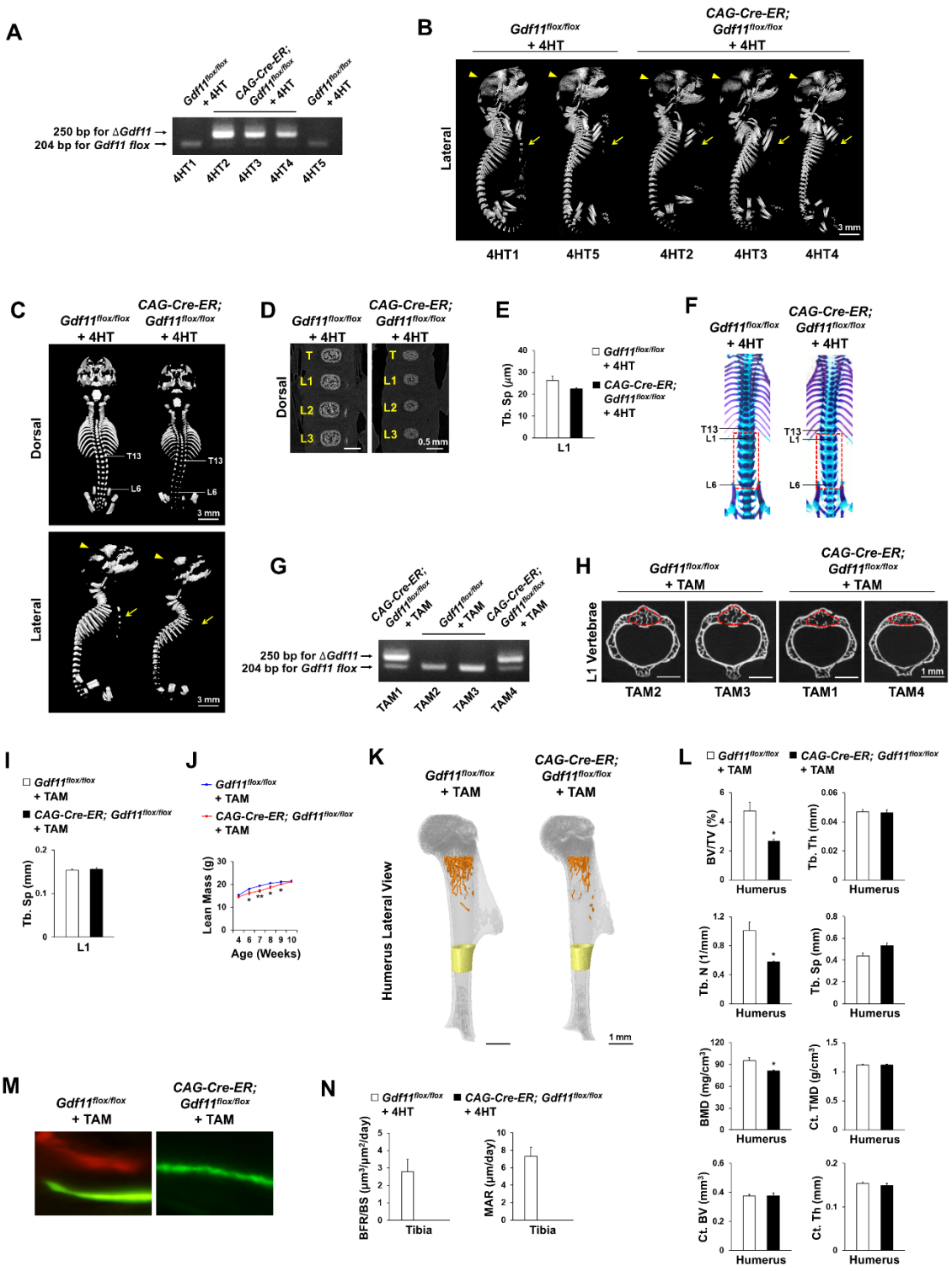

Fig. S2. Time-specific deletion of *Gdf11* impairs bone development in both E18.5 embryos and young adult mice. (*A*) Genotype results from livers of E18.5 littermates exposed to 4-hydroxytamoxifen (4-HT). The presence of *Gdf11* deletion band indicates successful recombination.

(*B*) Representative microCT images (scanned with Skyscan) of the E18.5 littermates genotyped in (*A*). Yellow arrowheads and arrows indicate calvarial bones and sterna, respectively. Note that 4-HT-treated *CAG-Cre-ER; Gdf11*$^{flox/flox}$ mice exhibit decreased mineralization in the skulls and sterna compared to their littermate controls. (*C*) Representative microCT images (scanned with Inspexio) of embryos at E18.5. Yellow arrowheads and arrows indicate calvarial bones and sterna, respectively. (*D*) Raw microCT cross section images (scanned with Skyscan) of E18.5 embryo vertebrae. (*E*) Supplemental microCT histomorphometric analysis (Tb. Sp, Trabecular separation) to Fig. 2*C*. (*F*) Alcian blue/alizarin red staining of vertebral columns of embryos at E18.5. Boxed regions indicate lumbar vertebrae. Note that conditional knockout mice display normal skeletal patterning, but smaller alizarin red-stained areas along the vertebral column. (*G*) Genotype results from the tails of male littermates injected with tamoxifen (TAM) for 5 consecutive days. The presence of *Gdf11* deletion band indicates successful recombination. (*H*) Raw microCT cross section images (scanned with Skyscan) of the 1st lumbar vertebrae (L1) of littermates genotyped in (*G*). Red lined regions indicate the regions of interest (ROI). (*I*) Supplemental microCT histomorphometric analysis (Tb. Sp, Trabecular separation) to Fig. 2*F*. (*J*) Supplemental DXA analysis (lean mass) to Fig. 2*G*. (*K*) Representative microCT images of 6-week-old mouse humerus. Trabecular bones are colored in orange and cortical bones are colored in yellow. (*L*) Histomorphometric analysis of microCT images (n = 4 for *Gdf11*$^{flox/flox}$ mice and n = 3 for *CAG-Cre-ER; Gdf11*$^{flox/flox}$ mice). (*M*) Representative calcein-alizarin red-labeled images of 6-week-old mouse L1. (*N*) Histomorphometric analysis of calcein-alizarin red-labeled images (n = 3 for *Gdf11*$^{flox/flox}$ mice and n = 3 (only single label detected) for *CAG-Cre-ER*; *Gdf11*$^{flox/flox}$ mice). BFR/BS, bone formation rate per bone surface; MAR, mineral apposition rate. All Scale bars are displayed with actual size values.

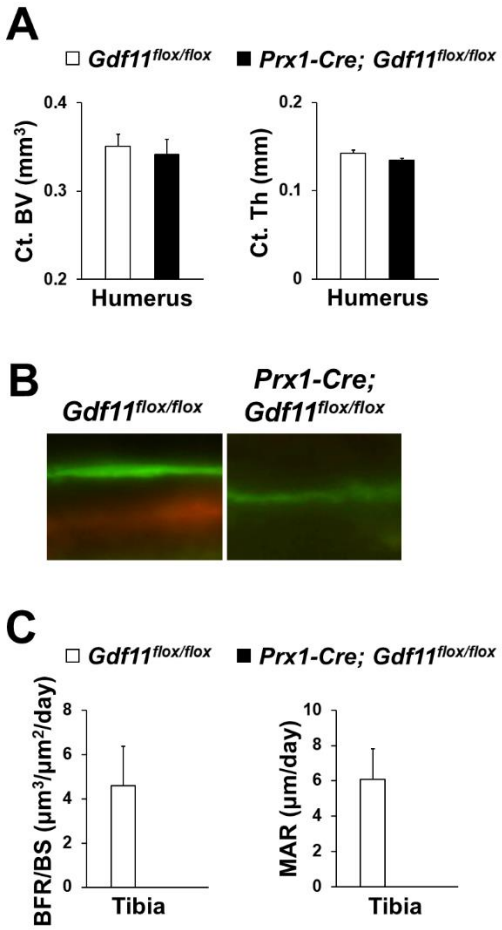

Fig. S3. *Prx1-Cre*-mediated *Gdf11* deletion leads to reduced bone mass in young adult mice. (*A*) Supplemental microCT histomorphometric analysis (Ct. BV, cortical bone volume; Ct. Th, cortical bone thickness) to Fig. 3*B*. (*B*) Representative calcein-alizarin red-labeled images of 5-week-old mouse tibia. (*C*) Histomorphometric analysis of calcein-alizarin red-labeled images of 5-week-old mouse tibia (n = 2 for *Gdf11*$^{flox/flox}$ mice and n = 3 (only single label detected) for *Prx1-Cre; Gdf11*$^{flox/flox}$ mice). BFR/BS, bone formation rate per bone surface; MAR, mineral apposition rate.

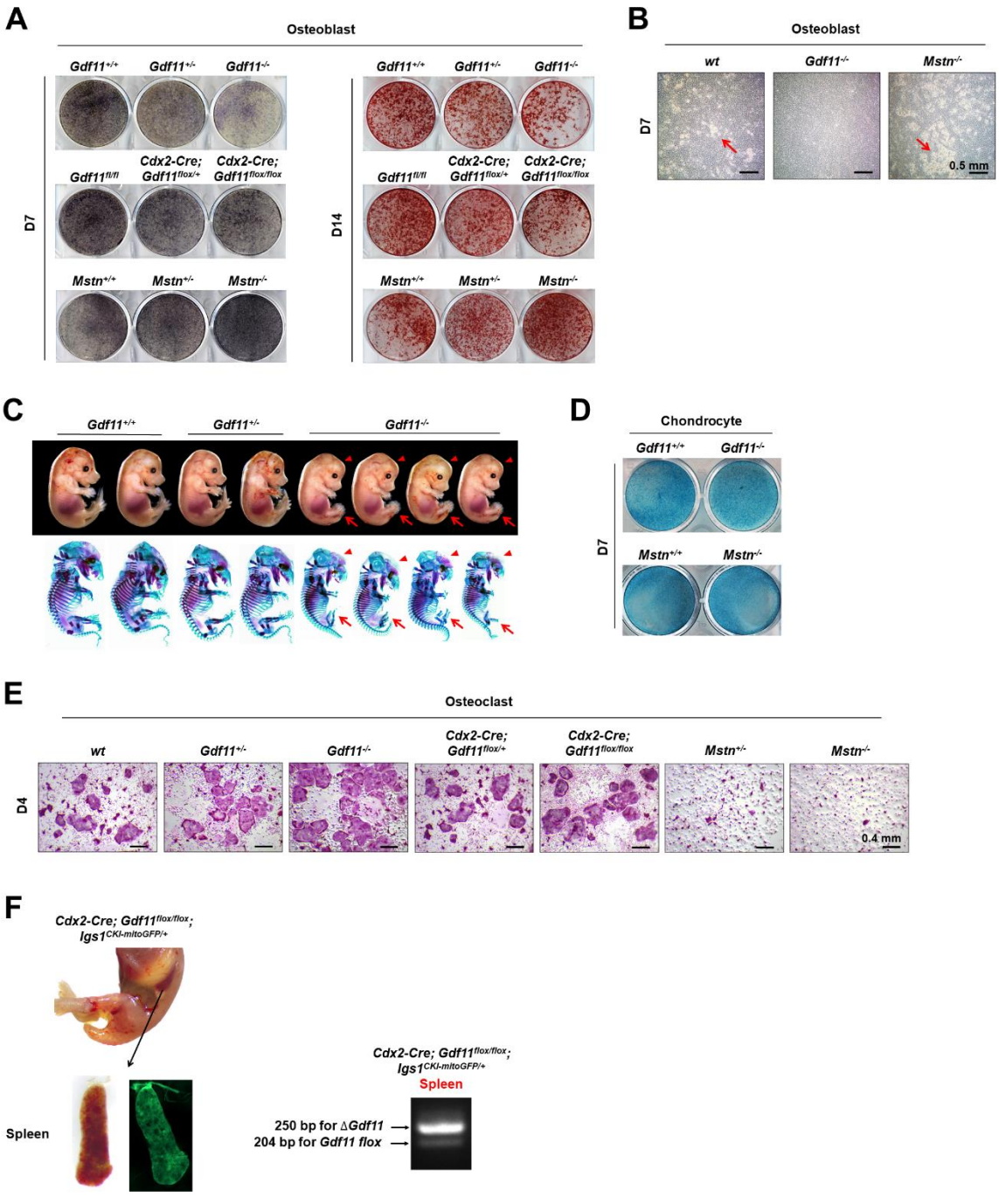

Fig. S4. *Gdf11* deletion, in contrast to *Mstn* deletion, impairs osteoblast differentiation and chondrocyte maturation, and stimulates osteoclast formation. (*A*) Alkaline phosphatase (ALP) and alizarin red S (ARS) staining of calvaria-derived osteoblasts (OBs) of newborn mice after 7 and 14 days of differentiation, respectively. (*B*) Raw images of osteoblasts viewed under light microscope after 7 days of differentiation. Red arrows indicate depositions of collagenous matrix. (*C*) Alcian

blue/alizarin red staining of E15.5 littermate embryos. Red arrowheads and arrows indicate underdeveloped skulls and hindlimbs of *Gdf11*$^{-/-}$ embryos, respectively. (*D*) Alcian blue staining of costal cartilage-derived chondrocytes (CHs) of newborn mice after 7 days of differentiation confirms the chondrocytic nature of the cells. (*E*) Tartrate-resistant acid phosphatase (TRAP) staining of spleen-derived osteoclasts (OCs) after 4 days of differentiation. (*F*) Spleen of newborn *Cdx2-Cre; Gdf11*$^{flox/flox}$*; Igs1*$^{CKI\text{-}mitoGFP/+}$ mouse. Cells expressing *Cdx2-Cre* are marked by GFP expression. All scale bars are displayed with actual size values.

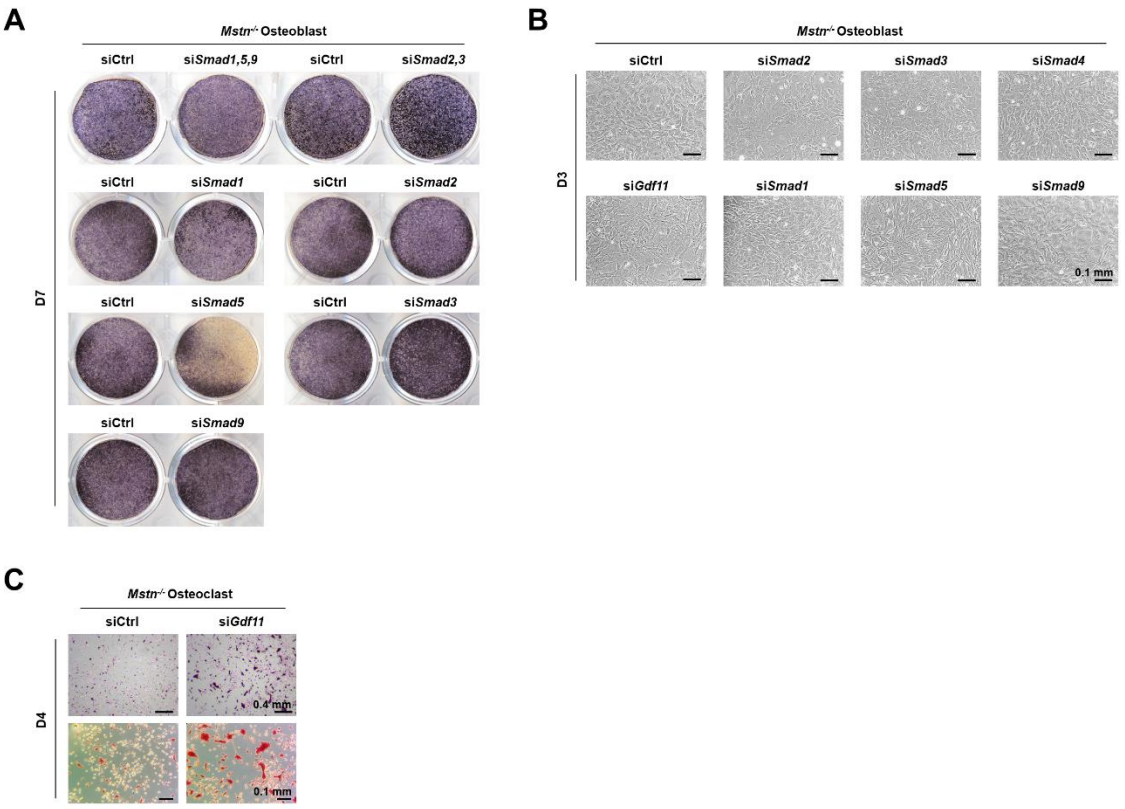

Fig. S5. *Gdf11* knockdown impairs differentiation of *Mstn*$^{-/-}$ osteoblasts, while stimulating differentiation of *Mstn*$^{-/-}$ osteoclasts. (*A*) Representative images of alkaline phosphatase (ALP) staining of *Mstn*$^{-/-}$ osteoblasts 7 days after *Gdf11*, *Smad1&5&9*, *Smad2&3*, or individual *Smad1, -2, -3, -4, -5, -9* knockdown. (*B*) Raw images of osteoblasts viewed under light microscope after 3 days after *Gdf11* or individual *Smad1, -2, -3, -4, -5, -9* knockdown. (*C*) Representative images of tartrate-resistant acid phosphatase (TRAP) staining of *Mstn*$^{-/-}$ osteoclasts 4 days after *Gdf11* knockdown. All scale bars are displayed with actual size values.

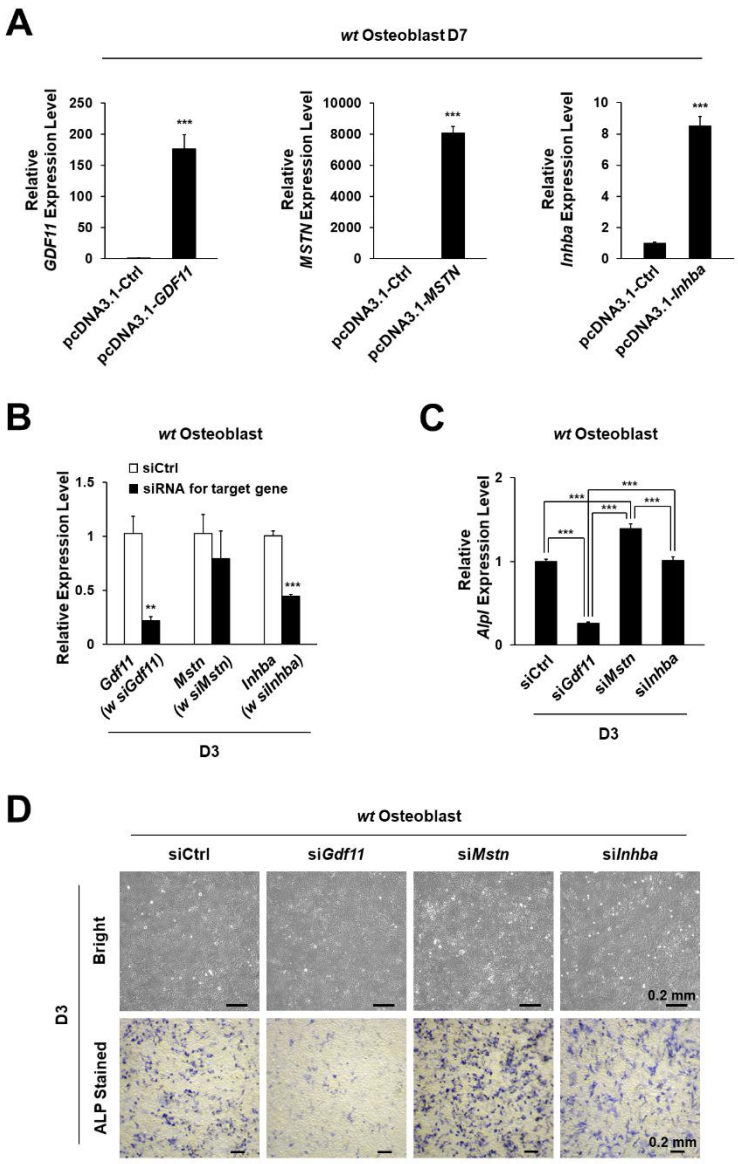

Fig. S6. *GDF11* overexpression stimulates osteogenic differentiation through the BMP signaling pathway. (*A*) Quantitative RT-PCR analysis of *GDF11*, *MSTN*, and *Inhba* expression in *wt* osteoblasts (OBs) at day 7 of overexpression (n = 4 each). (*B*) Quantitative RT-PCR analysis of *Gdf11*, *Mstn*, and *Inhba* expression in *wt* OBs at day 3 of knockdown of target genes (n = 3 each). (*C*) Quantitative RT-PCR analysis of *Alpl* expression in *wt* OBs at day 3 of knockdown of target genes (n = 3 each). (*D*) Representative images of raw (upper panel) and alkaline phosphatase (ALP)-stained (lower panel) *wt* osteoblasts at day 3 of knockdown of target genes. Data (*A*) and (*B*) represent mean ± SEM. *P < 0.05, **P < 0.01, and ***P < 0.001 by t test. Data (*C*) represent mean ± SEM. *P < 0.05, **P < 0.01, and ***P < 0.001 by ANOVA with Tukey's *post hoc* test. All scale bars are displayed with actual size values.

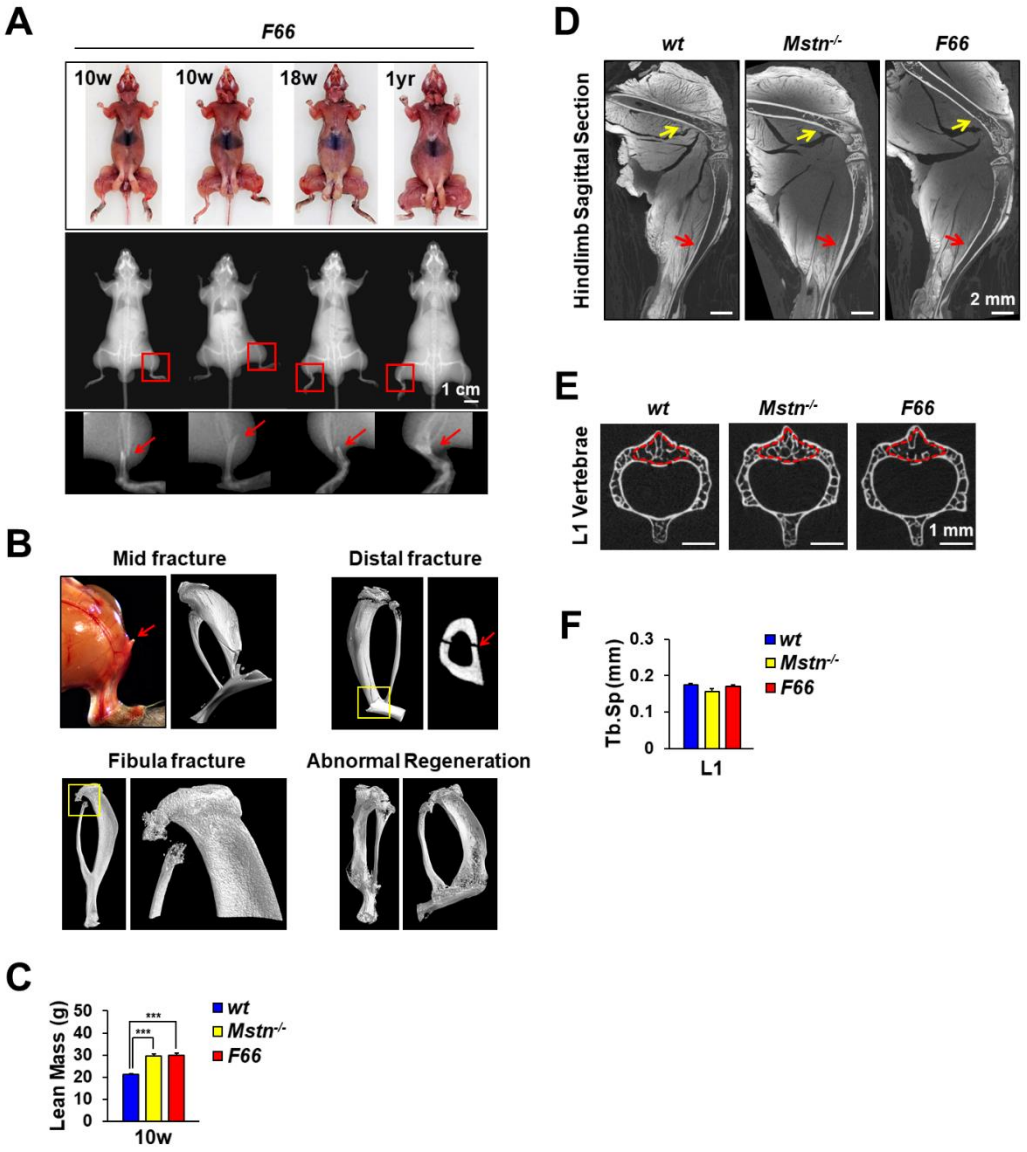

Fig. S7. FST overexpression leads to frequent tibia/fibula fractures. (*A*) Images of *F66* mice with tibia fractures at different ages. Boxed regions in DXA images (middle panel) are magnified to display fractured bones, which are pointed by red arrows (bottom panel). (*B*) MicroCT images (scanned with Skyscan) show various forms of fractures and abnormal regeneration in distal hindlimbs of *F66* mice. (*C*) Supplemental DXA analysis (lean mass) results to Fig. 7*C*. (*D*) Raw microCT cross section images (scanned with Skyscan) of the hindlimbs of 10-week-old mice. Note that while muscle mass is increased in both *Mstn*$^{-/-}$ and *F66* mice compared to *wt* mice, bone mass is increased only in *Mstn*$^{-/-}$ mice as indicated by yellow (femur) and red (tibia) arrows. (*E*) Raw microCT cross section images (scanned with Skyscan) of the 1st lumbar vertebrae (L1) of 10-week-old mice. Red lined regions indicate the regions of interest (ROI). (*F*) Supplemental microCT histomorphometric analysis (Tb. Sp, Trabecular separation) to Fig. 7*H*. All scale bars are displayed with actual size values.

Table S1. Quantitative RT-PCR primer sequences

Gene	Primer sequence (5'-3')
Runx2	F: TTCTCCAACCCACGAATGCAC
	R: CAGGTACGTGTGGTAGTGAGT
Sp7	F: CGCATCTGAAAGCCCACTTG
	R: CAGCTCGTCAGAGCGAGTGAA
Alpl	F: CCAACTCTTTTGTGCCAGAGA
	R: GGCTACATTGGTGTTGAGCTTTT
Bglap	F: CTGACAAAGCCTTCATGTCCAA
	R: GCGCCGGAGTCTGTTCACTA
Ibsp	F: CAGGGAGGCAGTGACTCTTC
	R: AGTGTGGAAAGTGTGGCGTT
Spp1	F: ATCTCACCATTCGGATGAGTCT
	R: TCAGTCCATAAGCCAAGCTATCA
Col10a1	F: CCACCTGGGTTAGATGGAAAA
	R: AATCTCATCAAATGGGATGGG
Ihh	F: CATGACCCAGCGCTGCAAGG
	R: CCTGGAAAGCTCTCAGCCGG
Nfatc1	F: GGAGAGTCCGAGAATCGAGAT
	R: TTGCAGCTAGGAAGTACGTCT
Fos	F: CGGGTTTCAACGCCGACTA
	R: TTGGCACTAGAGACGGACAGA
Src	F: GAACCCGAGAGGGACCTTC
	R: GAGGCAGTAGGCACCTTTTGT
Acp5	F: CACTCCCACCCTGAGATTTGT
	R: CATCGTCTGCACGGTTCTG
Ctsk	F: GAAGAAGACTCACCAGAAGCAG
	R: TCCAGGTTATGGGCAGAGATT
Dcstamp	F: GACCTTGGGCACCAGTATTT
	R: CAAAGCAACAGACTCCCAAA
Bmp2	F: GGGACCCGCTGTCTTCTAGT
	R: TCAACTCAAATTCGCTGAGGAC
Bmp4	F: AGCCCGCTTCTGCAGGA
	R: AAAGGCTCAGAGAAGCTGCG
Bmp7	F: CCAAAGAACCAAGAGGCCC
	R: GCTGCTGTTTTCTGCCACACT
Smad1	F: CGCTCCACGGCACAGTTAAG
	R: GCCAGTTGATTTGCGAACAGAA
Smad5	F: TGCAGCTTGACCGTCCTTACC
	R: GCAGACCTACAGTGCAGCCATC
Smad9	F: CGATCATTCCATGAAGCTGACAA
	R: TGGGCAAGCCAAACCGATA
Smad2	F: AACCCGAATGTGCACCATAAGAA
	R: GCGAGTCTTTGATGGGTTTACGA
Smad3	F: GTCAACAAGTGGTGGCGTGTG
	R: GCAGCAAAGGCTTCTGGGATAA
Smad4	F: GGACGCCCTAACCATTTCCAG
	R:CTGCTAAGAGCAAGGCAGCAAAC
Gdf11	F: CAGTGGACTTTGAGGCTTTTGG

	R: TGATTGGGGACATCTTGGTAGG
Mstn	F: CAGCCTGAATCCAACTTAGGC
	R: ACCTCTTGGGTGTGTCTGTCA
Inhba	F: GATCATCACCTTTGCCGAGT
	R: TGGTCCTGGTTCTGTTAGCC
GDF11	F: GACCTACACGACTTCCAGGG
	R: TACTGCTGGGTCCGTCTCC
MSTN	F: GGAGAAGATGGGCTGAATCCG
	R: TAGAGGGTAACGACAGCATCG

Movie S1. MicroCT reconstruction of Lumbar 1 of 10-week-old *wt* mice. Trabecular bones are colored in orange.

Movie S2. MicroCT reconstruction of Lumbar 1 of 10-week-old *Mstn*$^{-/-}$ mice. Trabecular bones are colored in orange.

Movie S3. MicroCT reconstruction of Lumbar 1 of 10-week-old *F66* mice. Trabecular bones are colored in orange.

Full unedited gel for Fig. S2*A*

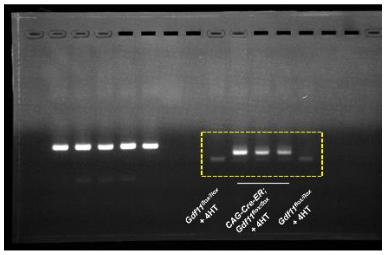

Full unedited gel for Fig. S2*G*

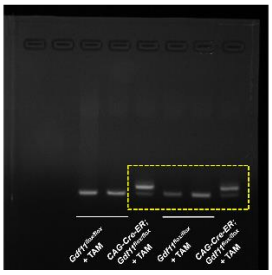

Full unedited gel for Fig. S3*F*

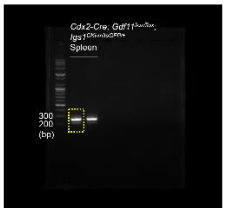

Unedited images of western blot for Fig. 4*F*

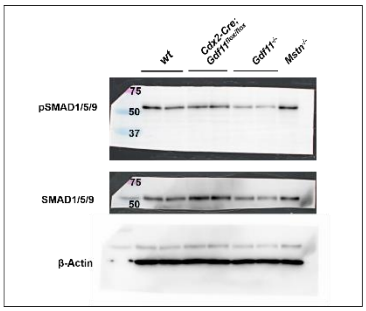

Unedited images of western blot for Fig. 6*D*

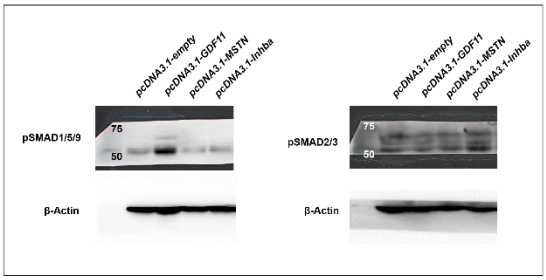

SI References

1. A. C. McPherron, T. V. Huynh, S. J. Lee, Redundancy of myostatin and growth/differentiation factor 11 function. *BMC Dev. Biol.* **9**, 24 (2009).
2. A. C. McPherron, A. M. Lawler, S. J. Lee, Regulation of skeletal muscle mass in mice by a new TGF-beta superfamily member. *Nature* **387**, 83-90 (1997).
3. S. J. Lee, A. C. McPherron, Regulation of myostatin activity and muscle growth. *Proc. Natl Acad. Sci. USA* **98**, 9306-9311 (2001).
4. J. P. Charles, O. Cappellari, A. J. Spence, J. R. Hutchinson, D. J. Wells, Musculoskeletal Geometry, Muscle Architecture and Functional Specialisations of the Mouse Hindlimb. *PLoS One* **11**, e0147669 (2016).
5. S. H. Lee, S. H. Lee, J. H. Lee, J. W. Park, J. E. Kim, IDH2 deficiency increases bone mass with reduced osteoclastogenesis by limiting RANKL expression in osteoblasts. *Bone* **129**, 115056 (2019).
6. S. E. Taylor, M. Shah, I. R. Orriss, Generation of rodent and human osteoblasts. *Bonekey Rep.* **3**, 585 (2014).
7. W. G. Cox, V. L. Singer, A high-resolution, fluorescence-based method for localization of endogenous alkaline phosphatase activity. *J. Histochem. Cytochem.* **47**, 1443-1456 (1999).
8. I. R. Orriss, M. O. Hajjawi, C. Huesa, V. E. MacRae, T. R. Arnett, Optimisation of the differing conditions required for bone formation in vitro by primary osteoblasts from mice and rats. *Int. J. Mol. Med.* **34**, 1201-1208 (2014).
9. A. J. Mirando, Y. Dong, J. Kim, M. J. Hilton, Isolation and culture of murine primary chondrocytes. *Methods Mol. Biol.* **1130**, 267-277 (2014).
10. M. Gosset, F. Berenbaum, S. Thirion, C. Jacques, Primary culture and phenotyping of murine chondrocytes. *Nat. Protoc.* **3**, 1253-1260 (2008).
11. I. Boraschi-Diaz, S. V. Komarova, The protocol for the isolation and cryopreservation of osteoclast precursors from mouse bone marrow and spleen. *Cytotechnology* **68**, 105-114 (2016).
12. A. C. McPherron, A. M. Lawler, S. J. Lee, Regulation of anterior/posterior patterning of the axial skeleton by growth/differentiation factor 11. *Nat. Genet.* **22**, 260-264 (1999).